



A modular focal plane detector system for the heavy ion reaction analyzer at NSC, New Delhi

D.O. Kataria^{a,*}, J.J. Das^a, N. Madhavan^a, P. Sugathan^a, A.K. Sinha^a, G. Dayanand^b,
M.C. Radhakrishna^b, A.M. Vinodkumar^c, K.M. Varier^c, Mahendrajit Singh^d,
N.V.S.V. Prasad^e

^aNuclear Science Centre, New Delhi 110067, India

^bDepartment of Physics, Bangalore University, Bangalore 560050, India

^cDepartment of Physics, Calicut University, Calicut 673635, India

^dDepartment of Physics, B.H.U., Varanasi 221005, India

^eDepartment of Nuclear Physics, Andhra University, Visakhapatnam 530003, India

Received 20 June 1995; revised form received 2 October 1995

Abstract

A detector system has been developed for the focal plane of the HIRA. It consists of two independent detectors, a low-pressure multiwire proportional counter (LP-MWPC) followed by a split-anode ionization detector. Details of the design and test results are presented. Using slow preamplifiers, the position resolution is ≥ 1 mm and the time resolution is estimated to be 1.5 ns for the LP-MWPC. The ionization detector gives 2.4% energy resolution for 150 MeV ^{28}Si scattered off a gold target and the $\Delta Z/Z$ obtained for $^{28}\text{Si}+^{27}\text{Al}$ is 1/42 for $Z=14$. Some results for fusion and transfer studies for the $^{48}\text{Ti}+^{58}\text{Ni}$ and $^{28}\text{Si}+^{68}\text{Zn}$ systems, respectively, at energies around the Coulomb barrier, are presented to highlight the performance of the detector system.

1. Introduction

Recoil mass spectrometers (RMS) are versatile tools for heavy ion reaction studies [1,2]. Coupled to a high rejection for beam-like particles is the excellent mass resolution with large solid angle, and space and energy focusing. They are ideally suited for studying reactions which are forward peaked and have found good application in the study of fusion and transfer reactions around the Coulomb barrier, spectroscopy by residue tagging, etc. The heavy ion reaction analyzer (HIRA) at the Nuclear Science Centre is a large solid angle RMS, details of which are presented elsewhere [3]. An important part of such spectrometers is the focal plane detector system (see Refs. [4,5] and references therein). At the focal plane, the HIRA brings to focus particles of varying values of “ M/q ” at different positions, with the length of the focal plane being ≥ 150 mm. The energy acceptance is $\pm 20\%$ and the mass acceptance is $\pm 5\%$, with a variable dispersion ranging from 10 to 40 mm/%. For the kind of focal plane described above, a detector system with the following features would be desirable:

1. cover the full focal plane area,

2. provide X and Y position with 1 mm resolution,
3. give a fast time signal for time-of-flight measurements, which can be used to extract energy and also to remove the (M/q) ambiguity,
4. give a reasonably good ΔE signal,
5. measure total energy,
6. measure Z whenever possible,
7. have a reasonably large dynamic range, and
8. have minimum material in the path of the incoming particle.

Since a detector system of this type would have to be a combination of detectors, it would be desirable to have it modular to increase its versatility and make it easier to handle. We have designed, fabricated and tested a detector system satisfying the above requirements. It consists of a 2-D position sensitive low-pressure multiwire proportional counter [6] and a split-anode transverse ionization detector. The system is designed so that each of the detectors can be operated independently or as a composite system.

2. Test detector

Before undertaking the fabrication of the MWPC for HIRA, it was decided to fabricate a smaller prototype

* Corresponding author.

detector of the same type. A test detector with an active area of 45 mm×45 mm was fabricated for this purpose. The detector is a parallel grid avalanche detector. The electrodes are two grids of 0.5 mm spaced 25 μ m wires, soldered to two sides of a 1.6 mm thick double sided G-10 PCB. The windows are 2 μ m plain mylar foils. One of the electrodes is kept at high voltage whereas the other is grounded through a 50 Ω resistor, across which the signal is observed.

The detector was tested with 3–8 Torr isobutane at voltages varying from 350 to 600 V. Using a fast preamp, signals of the order of 3–5 ns rise time were observed. In combination with a partially depleted F-series surface barrier detector, 1 ns time resolution was obtained. The detector gave similar performance with fission fragments obtained by bombarding oxygen ions onto a bismuth target. An energy signal was also extracted from the detector in order to study its ability to discriminate between the heavy fission fragments and the lighter beam-like particles. The spectrum obtained is shown in Fig. 1.

The detector was designed such that it can be made position sensitive by replacing the PCB with another one where the wires can be connected to a resistor chain or to the taps of a delay line chip. This was done by fabricating a PCB which consisted of three grids of 1 mm spaced 25 μ m wires. The interelectrode spacing is 1.6 mm. The wires on the central and one of the outer electrodes are connected to stripes, centre to centre spacing 3 mm, with the two grids running orthogonally to each other. These give the X and Y position. The third electrode can be used for timing and/or ΔE . Connections to the electrodes are made such that high voltage and ground electrodes can be chosen as desired. The stripes are connected to a resistor chain,

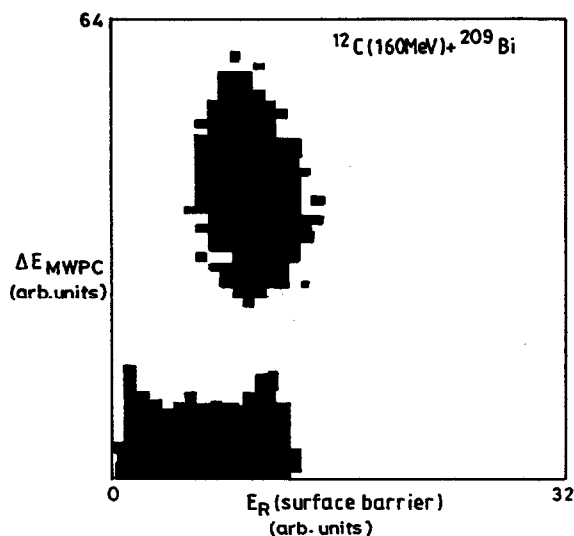


Fig. 1. Multiparameter plot of energy deposited in the MWPC versus energy deposited in the surface barrier detector.

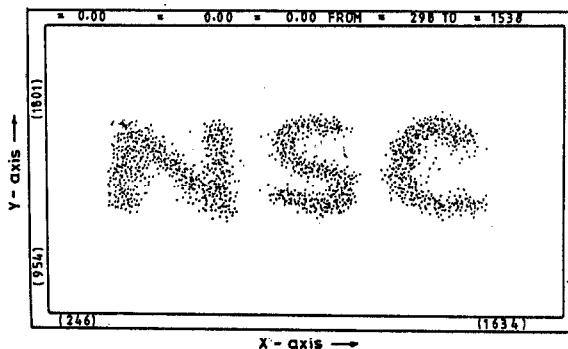


Fig. 2. Software processed spectrum obtained by masking the MWPC with aluminium foil with ‘NSC’ cut out and using a ^{252}Cf source. Width of the opening for the letters is 1 mm.

one end of which is capacitively coupled to ground and the signal is observed from the other end.

The detector was operated with 4 Torr isobutane gas at a voltage of -450 V on the outer electrode and -225 V on the central electrode. Using a ^{252}Cf source and a mask with 1 mm wide slits, the FWHM obtained was 1.3 mm. Using a mask with ‘NSC’ cut out, the software processed spectrum obtained is shown in Fig. 2.

The design of the detector is modular. Each frame is an electrode or a window frame, making the detector quite compact. However, this design restricted ease of replacement of the electrodes or windows and also restricted modifications. As the detector was to adapt to the outlet flange at the focal plane, where there is sufficient space and it is not essential that the detector be compact, for the large area detector, the design was modified.

3. Large area MWPC

A schematic diagram of the detector is shown in Fig. 3. The housing is a 350 mm×300 mm, rectangular SS flange, 30 mm thick, with a 245 mm diameter step cut out. The step is sufficient to accommodate rectangular electrode frames which provide an active area of 190 mm×60 mm. The larger dimensions for the flange are required so that it can couple to a rectangular chamber of matching dimensions, 50 cm deep, following the MWPC. A pumping station is provided between the exit flange of the HIRA and the MWPC. The entrance window is a 1.5 μ m thick aluminized mylar foil, glued onto a 6 mm thick G-10 frame with a 190 mm×60 mm slot cut out. The window frame is attached to the exit of the pumping station. 70 μ m tungsten wires spaced 10 mm apart, vertically as well as horizontally, glued along with the foil, provide support to the window to withstand pressure. The exit window frame has identical dimensions but is made of 15 mm thick SS and the slot is 135 mm×35 mm. It also forms the entrance window to the ionization detector following the MWPC.

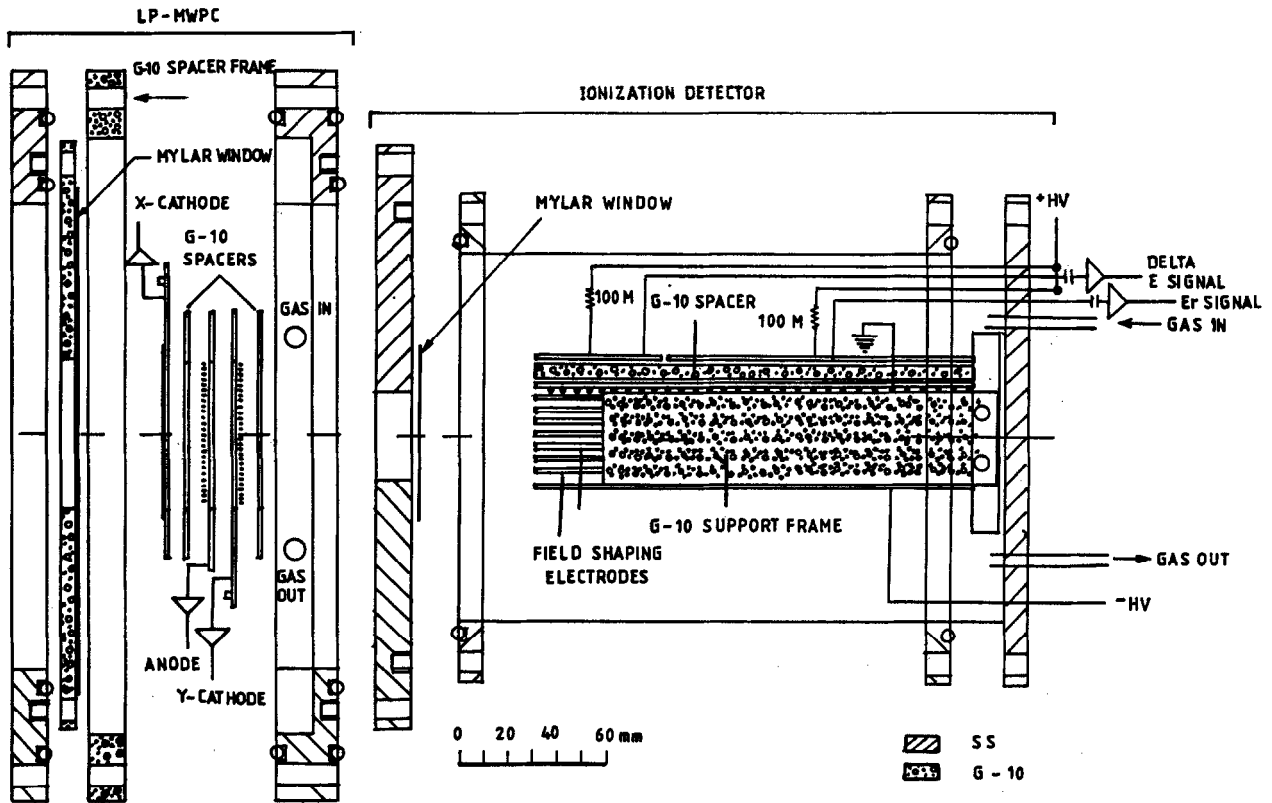


Fig. 3. Schematic diagram of the detector system.

The MWPC is electrically isolated from the pumping station with the help of a 15 mm thick G-10 frame.

The active volume consists of three electrodes, an anode sandwiched between two cathodes. The electrode frames are 1.6 mm thick G-10 PCBs. Grids of 25 μm gold plated tungsten wires, spaced 1 mm apart, are soldered to the frames. A spacing of 3.2 mm is maintained between the electrodes by using 1.6 mm thick unclad PCBs as spacers. The central electrode, the anode, has all the wires interconnected and provides the time and ΔE signal. The detector is made position sensitive using the delay line technique. The delay lines used are chips from Peizo Electric, model PE 21173, having nine taps, 40 ns delay per chip and with 100 Ω characteristic impedance.

On the X-sensing cathode, each wire is connected to the tap of a delay line. A double sided printed circuit board, with plated through holes, had to be used in order to accommodate the high density of lines. The aim was to minimize the differential nonlinearity and achieve better than 1 mm position resolution. Requirements for position resolution in the Y-direction are not that stringent and, hence, on the Y-sensing cathode, three wires were interconnected and then connected to a delay line tap. Signals can be taken from the two ends of the delay line chain. 100 Ω resistances are connected to ground at the two ends of the chain for impedance matching.

4. Ionization detector

A schematic representation of the detector is shown in Fig. 3. The detector housing is a 150 mm diameter cylinder. The entrance flange has been described earlier. Two 6 mm thick G-10 bars, 37 mm \times 200 mm, are mounted along their breadth onto the back flange using aluminium L-channels. The electrodes, made of 1.6 mm thick G-10 PCBs, are 135 mm wide and 185 mm deep, and are mounted lengthwise onto the G-10 bars. The grid-cathode and grid-anode spacings are 40 and 6 mm, respectively. The grid is a nickel mesh with 89.5% transmission, soldered to the PCB frame. The anode is split into two sections along the depth of the detector. The mounting is such that it is possible to change the depths without much difficulty. For initial tests, the depths were 9 cm for the ΔE and 9.5 cm for the E_R . These were later changed to 5 and 13.5 cm, respectively.

There is provision to mount PCBs along the side faces of the bars and at the front as well as the back of the detector active volume. Using these mountings, either a Faraday cage arrangement or field shaping can be provided. The former arrangement was used in the initial tests. However, since this does not provide a uniform field over the full active area and could lead to degradation of the resolution at the edges, we changed to the latter. BNC and

Lemo vacuum feedthroughs are provided on the back flange to carry the signals out and there is also a provision for gas inlet and outlet on the back flange. Additionally, a mounting arrangement is provided on the back flange for mounting a 2-D position sensitive surface barrier detector.

5. Electronics

The electronics block diagram is shown in Fig. 4. For the LP-MWPC, positive HV is supplied to the central electrode, the anode, while the outer electrodes are grounded. The anode is connected to a charge sensitive preamplifier (EG&G Ortec 142A, which gives a timing as well as energy signal). On the cathodes, one end is connected to the 142A, while the other end is terminated through a 50 Ω resistor. Fast timing preamplifiers, like the VT 120 from EG&G Ortec, have also been used to obtain the optimum timing (<5 ns rise time), but it was not then possible to obtain a ΔE signal from the same preamplifier. The time signals are fed to CFDs (EG&G Ortec 935). For the position measurement, the time signal from the anode is used to start the TAC while the stop signal comes from the cathode through a delay. A TAC range of 1 μ s and 100 ns is used for the measurement of the X and Y position, respectively. The ΔE signal is fed to a spectroscopy amplifier. The TAC and amplifier signals are carried to the ADC (EG&G Ortec AD811) and the strobe to the ADC is derived from the anode CFD output.

The preamplifiers for the ionization detector were fabricated at NSC using the CS507 [7] preamplifier chip. They were then mounted inside the detector volume in order to minimize the cable length from the electrodes to the preamplifier input. This gave a better signal-to-noise ratio. However, possibly due to improper heat dissipation, some of the resistors burnt off, which caused the noise to worsen. Under these conditions, the signal-to-noise ratio for the EG&G Ortec 142A preamp, when placed outside

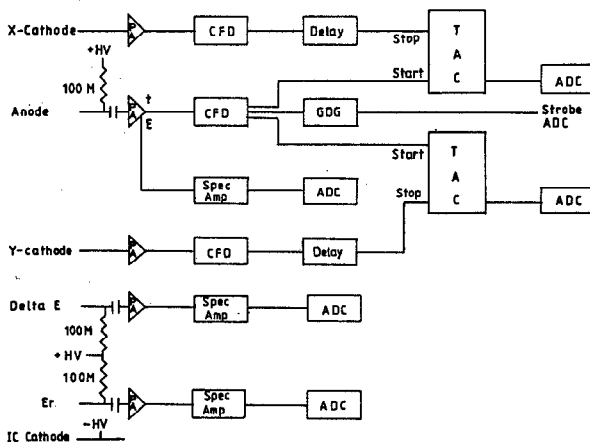


Fig. 4. Block diagram of the electronics for the detector system.

the detector, turned out to be better and so the CS507 preamplifiers were eventually removed. The signals from the preamplifiers were fed to spectroscopy amplifiers, with a shaping time of 2 μ s, and subsequently to the ADC. The gating is provided by the PPAC anode signal as described earlier.

6. Test and performance

6.1. MWPC

The detector was initially tested with a ^{252}Cf source at 6 Torr and 520 V on the anode. The anode signals observed from EG&G Ortec VT120 preamplifiers showed approximately 5 ns rise time. In order to obtain an energy signal in addition to the time signal, we eventually used a charge sensitive preamplifier, the EG&G Ortec 142A. The rise time observed with this was approximately 20 ns.

The detector was then masked by a slit structure consisting of 1 mm wide slits, 10 mm long, running horizontally as well as vertically. The response of the detector has been found to be quite linear in position with a position resolution ≥ 1 mm. A rigorous test for time resolution has not been carried out using a source. However, an estimate is obtained from the $^{28}\text{Si} + ^{68}\text{Zn}$ experiment, described in Section 7. After correcting for target thickness, kinematic broadening and width of the pulsed beam, the resolution was estimated to be less than 1.5 ns, assuming the time spread through the spectrometer to be around 0.5 ns. Both the time and position resolution can be improved by using fast preamplifiers.

Assuming 100% efficiency for the ionization detector mounted behind the MWPC, which was independently verified as described in Section 6.2, the efficiency for the MWPC can be determined. For the ^{252}Cf source, 100% efficiency for the fission fragments is obtained by operating the detector at 5 Torr and 550 V. This is the operating pressure for most of the beam runs where it is additionally checked online to ensure 100% efficiency.

Beam tests

The detector was used in an experiment to study sub-barrier fusion cross-sections for the reaction $^{48}\text{Ti} + ^{58,60,64}\text{Ni}$, at energies around the Coulomb barrier. The HIRA was set for the recoiling evaporation residues and the detector was operated at 4 Torr, with 450 V on the anode. The beam-like particles which do make it to the focal plane have to be separated out from the particles of interest. This can be achieved by doing a time-of-flight measurement with a start detector at the entrance of the HIRA or by using a pulsed beam. However, in some cases this can also be achieved by extracting a ΔE signal from the MWPC. In our case, we could obtain efficient separation by using the ΔE signal. Fig. 5 is a multi-parameter plot of ΔE vs X-position for fusion-evaporation residues

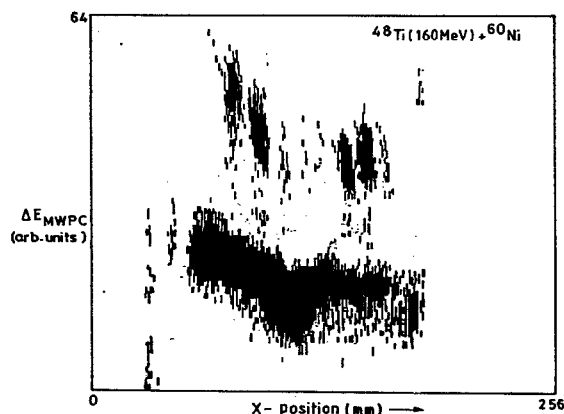


Fig. 5. Multi-parameter plot of energy deposited in the MWPC versus X-position at the focal plane for evaporation residues from (160 MeV) $^{48}\text{Ti}+^{60}\text{Ni}$.

from (160 MeV) $^{48}\text{Ti}+^{60}\text{Ni}$, indicating a good separation of the recoiling evaporation residues from the beam-like particles.

6.2. Ionization detector

After masking the detector with a PCB with a 10 mm hole in the centre, it was tested with a ^{252}Cf source, using isobutane gas. The operating voltage was maintained at 1.25 V/Torr cm for the grid–cathode region and 2.5 V/Torr cm for the grid–anode region [8]. The tests were carried out at different gas pressures. At 64 Torr and with the CS507 preamplifiers, the best resolution observed was 4%. With the EG&G Ortec 142A, the best resolution obtained was 2.7%. The efficiency was found to be 100% by comparing with a surface barrier detector subtending the same solid angle.

6.2.1. Beam tests

The detector has also been tested with a 150 MeV ^{28}Si beam. For this test, the anode was split into two sections, 9 and 9.5 cm deep, providing ΔE_1 and ΔE_2 , and a 2-D position sensitive strip detector [9] was mounted at the back providing E_R . The detector was mounted on the 20° port of the general purpose scattering chamber at NSC [10]. An aluminium sheet, with a 20 mm hole in the centre, was mounted on a movable arm in front of the detector to mask the detector and allow scanning of different regions. Using a gold target, the energy resolution, for operating parameters the same as for the source test, was 2.4%. No corrections have been made for target thickness, kinematic broadening or entrance foil thickness. The detection efficiency for the heavy ions was verified to be 100% by comparing with counts in the strip detector at the back. For Z identification, an aluminium and a nickel target were used. The spectrum obtained with the aluminium target is

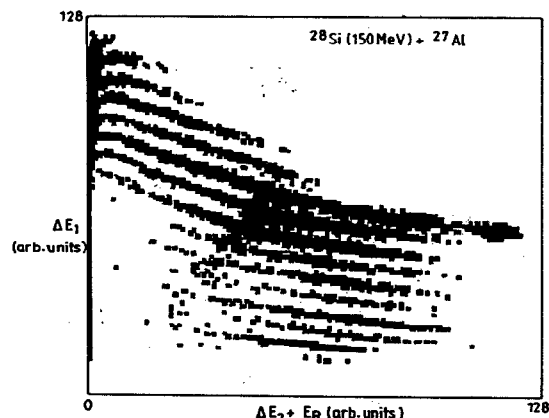


Fig. 6. ΔE_1 vs $(\Delta E_2 + E_R)$ spectrum for (150 MeV) $^{28}\text{Si}+^{27}\text{Al}$ with the detector placed at 20° . Symbols are described in the text.

shown in Fig. 6. The $\Delta Z/Z$ obtained is around $1/42$ for $Z=14$.

7. Detector system in conjunction with the HIRA

A pumping station has been provided at the focal plane chamber, the exit of which is a rectangular flange compatible with the dimensions of the MWPC. The window frame is mounted on this flange. At the exit of the MWPC, an identical frame provides the exit window. The ionization detector entrance window flange also has the same dimensions. Hence, whenever both the detectors are to be used in conjunction, the MWPC exit window frame is replaced by the ionization detector. This eliminates an extra window in the path of the ions. In some applications, the second window may also be removed and both the detectors could be operated at the same pressure.

This configuration has been used to study fusion products from $^{32,34}\text{S}$ on $^{46,48,50}\text{Ti}$, at energies around the barrier, using a 3 ns wide pulsed beam. The flight time of the recoils is of the order of 600 ns. We have used a beam pulse interval of 250 ns as well as $1\ \mu\text{s}$. The energy vs time-of-flight spectrum obtained for the latter is shown in Fig. 7, where it can be seen that with the help of the ionization detector, a clean separation can be obtained between the recoils of interest and beam-like particles reaching the focal plane. A similar separation can also be obtained by using the energy signal from the MWPC, but this is not as clean. No separation is possible, however, using the ionization detector ΔE vs E information.

In another experiment, a pulsed, 78 MeV, ^{28}Si beam was bombarded onto a ^{68}Zn target. For this case, the energy of the Zn-like recoils may be high enough for Z-identification. However, due to energy losses in the two mylar foils and the target, the final energy is much lower. Hence, Z is not determined, although separation between beam-like and recoils is obtained. In addition, using the pulsing

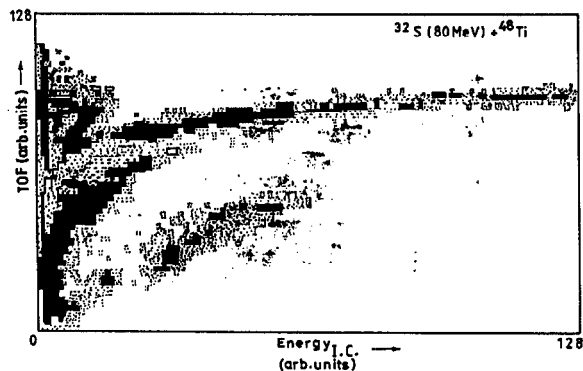


Fig. 7. Energy versus time-of-flight spectrum for the particles produced in the fusion-evaporation reaction of an 80 MeV, pulsed, ^{32}S beam incident on a ^{48}Ti target.

system RF and the timing signal from the MWPC, the TOF of the recoils is recorded. A multi-parameter spectrum displaying TOF vs position at the focal plane, gated for the recoils using the TOF vs energy information, is shown in Fig. 8. The M/q ambiguity is clearly resolved using the TOF information obtained from the MWPC and pulsing system.

One of the problems encountered with the system is the smaller size of the ionization detector, whereby all the recoils do not go into the back detector. The active area of the ionization detector is 120 mm \times 35 mm, whereas the HIRA can disperse recoils up to 150 mm \times 40 mm. About 15% of the recoils have been found to be missed in some experiments due to this. Another limitation is the depth of the detector, due to which the ion counter has to be operated at higher pressures. Since the MWPC timing performance deteriorates at higher pressures, this does not

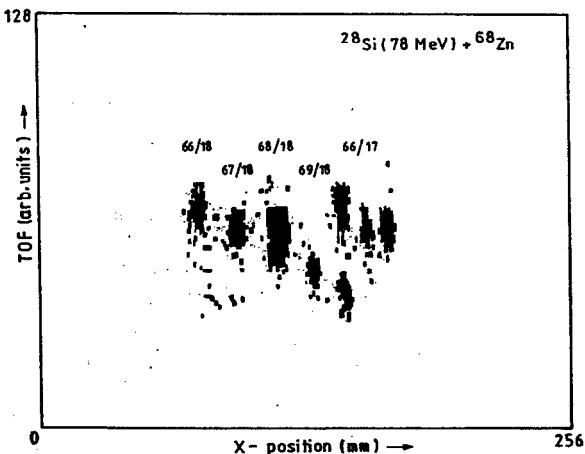


Fig. 8. Time-of-flight versus X-position at the focal plane, gated for recoil particles, for the transfer reaction of 78 MeV ^{28}Si incident on a ^{68}Zn target. The TOF is obtained using the pulsing system RF and timing from the MWPC.

allow operation of the two detectors in the same gas volume.

8. Summary

A focal plane detector system has been fabricated and used in a number of experiments with the HIRA. It consists of a low-pressure multiwire proportional counter and a split-anode ionization detector. Using slower charge sensitive preamplifiers, the time and position resolution of the MWPC has been estimated to be ≤ 1.5 ns and ≥ 1 mm, respectively, which has been found to be sufficient for most applications with the HIRA. The resolutions can be improved by going back to fast preamplifiers. The energy resolution has been found to be 2.4% for ^{28}Si scattered off a gold target, without any corrections incorporated. With products from $^{28}\text{Si}+^{27}\text{Al}$, the $\Delta Z/Z$ is 1/42 for $Z=14$.

Using the detector system with the HIRA no Z-identification has been possible for the systems studied, due to the low specific energies of the ions. However, the energy information from the ionization detector is used, in conjunction with time-of-flight, for beam rejection and for resolving the M/q ambiguity. Also, in some cases, the $\Delta E-E$ information is used for beam rejection. Separation of the beam-like particles from particles of interest has also been quite effective by using the ΔE signal from MWPC, in particular for the fusion studies carried out at NSC.

Due to the smaller size of the ion counter, some recoils are missed. Also, due to the smaller depth, operation at low pressures is not possible. To overcome these problems, a larger ionization detector is being fabricated which is 450 mm deep and has an active area equivalent to the MWPC.

Acknowledgments

The authors would like to thank the Pelletron operations staff at NSC for providing stable beams for carrying out experiments with the detection system. Helpful discussions with Dr. A. Roy and support and guidance from Prof. G.K. Mehta are gratefully acknowledged.

References

- [1] H.A. Enge and D. Horn, Nucl. Instr. and Meth. 145 (1977) 271.
- [2] T.M. Cormier, M.G. Herman, B.S. Lin and P.M. Stwertka, Nucl. Instr. and Meth. 184 (1981) 423; Nucl. Instr. and Meth. 212 (1983) 185.
- [3] A.K. Sinha, N. Madhavan, J.J. Das, P. Sugathan, D.O. Kataria, A.P. Patro and G.K. Mehta, Nucl. Instr. and Meth. 339 (1994) 543.
- [4] K.E. Rehm and F.L.H. Wolfs, Nucl. Instr. and Meth. 273 (1988) 262.

- [5] A. Guerrieri, G. Maron, G. Montagnoli, D.R. Napoli and G. Prete, *Nucl. Instr. and Meth.* 299 (1990) 133.
- [6] A. Breskin, R. Chechik and N. Zwang, *Nucl. Instr. and Meth.* 141 (1977) 505; *Nucl. Instr. and Meth.* 165 (1979) 125.
- [7] Clear Pulse Co./Katsura Co. Ltd, Japan.
- [8] H.W. Fulbright, *Nucl. Instr. and Meth.* 162 (1979) 21.
- [9] Design W, Micron Semiconductor Limited, UK.
- [10] D.K. Avasthi, A. Tripathi, D. Kabiraj, S. Venkataramanan and S.K. Datta, NSC Technical Report, General Purpose Scattering Chamber, NSC/TR/DKA/92/16.